ASSESSING ELASTIC RECOVERY IN A STRETCH-SHORTENING TASK

ASSESSING THE INFLUENCE OF ELASTIC RECOVERY

IN A STRETCH-SHORTENING CYCLE TASK:

A MUSCLE MODELLING APPROACH

By

CHARLES STEPHEN LYNCH B.SC.

A Thesis

Submitted to the School of Graduate Studies

in Partial Fulfilment of the Requirements

for the Degree

Masters of Science

McMaster University

© Copyright by Charles S. Lynch, May 1992

MASTER OF SCIENCE (1992)   McMASTER UNIVERSITY

(Human Biodynamics)   Hamilton, Ontario

TITLE: Assessing the Influence of Elastic Recovery in a
         Stretch-Shortening Cycle Task: A Muscle Modelling
         Approach

AUTHOR: Charles Stephen Lynch, B.Sc. (Concordia University)

SUPERVISOR: Dr. James J. Dowling

NUMBER OF PAGES: ix, 70

ABSTRACT

A Hill-based muscle model was used to assess the influences of series elastic recovery in stretch-shortening cycle (SSC) contractions at the human elbow. Elbow torque, EMG and joint kinematics were recorded as eight male subjects performed a variety of elbow flexion and extension tasks. A significant performance enhancement was observed in SSC vs non-SSC elbow flexions (20% greater angular impulse).

The muscle model used activation-force, length-tension and force-velocity functions to estimate instantaneous elbow flexor and extensor moments. These moments were summed with a passive elbow moment to obtain estimates of net elbow moment and angular impulse. The estimated values were compared to actual measures of joint torque and angular impulse. The model accurately estimated the angular impulse generated by non-SSC contractions, but demonstrated substantial underestimation errors in SSC contractions.

The majority of the SSC performance enhancement could not be attributed to either neural potentiation or to a better exploitation of contractile component mechanics. Since the model was designed to account for these influences but did not possess an ability to account for series elastic recovery, the performance enhancement which was not accounted for by the

model was attributed to the recovery of strain energy stored in the SEC of the flexor muscles during the stretch phase.

Past studies of SSC enhancement in voluntary movements have been unable to discern between the influences of elastic recovery, neural potentiation and other SSC phenomena. The methods employed in this study permitted the influence of elastic energy recovery to be partitioned from a net SSC performance enhancement. The results indicate that elastic recovery can play an important role in human movement, and that Hill-based muscle models offer a useful tool for studying physiological phenomena which can not be isolated experimentally.

Acknowledgements

CONTENTS

List of Figures

List of Tables

1.0 INTRODUCTION

The stretch-shortening cycle (SSC) of muscular activity plays an important role in many human movements, particularly in athletics. This cycle consists of an active lengthening of a muscle or of a group of muscles, followed by an active shortening of those same muscles. The SSC is evident in running, jumping, throwing, kicking and numerous other activities; many of whose primary goal is to generate rapid displacements of one or more body segments.

Considerable evidence exists documenting the contributions of the SSC to the enhanced performance of these types of activities (for reviews see Cavagna, 1977; Shorten, 1987). This enhanced performance is typically defined as an increase in some mechanical parameter (e.g. force, velocity, work, power, efficiency...) during the concentric phase of the SSC activity, when compared to the same phase of similar activities performed without prior stretch.

The enhanced performance observed in SSC activities has been attributed to a variety of different phenomena. The most commonly cited cause for augmented performance is the utilization of strain energy which can be stored in the series elastic component (SEC) of muscle during the eccentric phase of the movement (Alexander & Bennett-Clark, 1977). Neural potentiation, observed as an increase in muscular activity and

presumably evoked by spinal reflexes, has also been postulated as a source of SSC enhancement (Bosco et al., 1982). In contrast to the above explanations, Van Ingen Schenau (1984) suggested that the SSC merely allows for less energy to be wasted in taking up the "slack" of a resting muscle. Most recently, the augmented performance has been explained as being partially, if not primarily due to a more optimal interaction between the neural drive to a muscle and the mechanics of muscular contraction (Hof and Van den Berg, 1986; Chapman, 1985; Dowling, 1992). That is, a SSC may allow a muscle to generate more force early in the shortening phase of a contraction, first of all because the force is allowed to build up during the active pre-stretch, and secondly because the series elastic component of the muscle may account for most of the change in muscle length, thus allowing the contractile component to shorten at slower velocities which are more optimal for force generation.

It is quite likely that, given suitable circumstances, each of the above mentioned phenomena can contribute to SSC enhancement. However, because of complex interactions between these influences, the magnitude and the relevance of their individual contributions is rather difficult to assess. In order to accurately measure the influence of any given SSC phenomenon on movement performance, a method must be used which can discriminate between the influences of the various

phenomena. The objective of this study was to develop such a method, that would be suitable for evaluating the influence of elastic recovery in some simple upper limb stretch-shortening cycle movements.

The methods employed in this study consisted, in part, of using a Hill-based muscle model to describe the internal and external mechanics of the movements. This chapter presents a review of some of the more pertinent literature relating to enhanced performance in SSC activities, along with a brief review of Hill-based muscle models. Following this, a detailed description of the purpose and rationale of the study is presented.

1.1 Stretch-Shortening Cycles in Human Movement

Stretch-shortening cycles are present in many human movements, both in athletics and in activities of daily living. In order to be classified as a SSC, a concentric action must be preceded by a counter-movement, and this counter-movement must be resisted by muscular effort. These conditions cause the muscles involved to be forcibly stretched just prior to shortening. The force causing the stretch is most often either the force of gravity or the effort of antagonist muscles. An example of a group of muscles which routinely undergo SSCs is the plantar flexor group during walking, running and jumping. Many upper limb muscles also undergo SSCs during lifting, throwing and striking tasks.

Because the SSC is common to so many human movements, its role in coordinating and enhancing movement performance has become a very appealing research topic in the fields of biomechanics and exercise physiology.

1.2 Evidence of Enhanced Performance in SSC Activities

The significance of the SSC in enhancing movement performance is indisputable. Initial attempts to quantify the influence of the SSC on human performance date back over a century, when Marey & Demeny (1885) examined the performance of successive vertical jumps. They found that the height obtained in a second jump was always higher than that obtained in the first jump. They attributed the enhanced performance of the second jumps to "storage of work in the tense muscles" during the landing from the first jump (Cavagna, 1977). Since then, many other studies have shown that a SSC improves movement performance in a wide variety of tasks.

1.2.1 Increased Force, Work, Speed and Power

Contemporary studies examining vertical jumps with and without counter-movements have shown increases in peak ground reaction forces, jump height, positive work performed, speed of the concentric phase and peak power (Komi, 1984; Bobbert & Van Ingen Schenau, 1988). Similar force and speed enhancement have also been observed in upper limb movements performed with and without previous stretch (Bober et al., 1980; Thomson and Chapman, 1988; Wilson et al., 1991).

Some of the earliest quantitative evidence of SSC enhancement was derived from a series of investigations performed by Giovanni Cavagna in the 1960's, to examine "elastic recovery" in isolated muscle preparations (Cavagna et al., 1964, 1965, 1968). In these studies, the work which could be performed by isolated frog sartorius muscle was found to be significantly greater when maximally stimulated from a forced stretch, than from an isometric state.

1.2.2 Increased Efficiency

A second form of enhanced performance which has been commonly observed in SSC movements is an increase in mechanical efficiency. Apparent mechanical efficiency can be defined as the ratio between work performed and the metabolic cost of performing that work (Cavagna, 1977). The maximal efficiency of transforming chemical energy into mechanical work by the contractile component of muscle is thought to be approximately 25 percent (Fenn, 1930). However, a number of studies have shown that the apparent mechanical efficiency of running can be as high as 30 to 80 percent depending on the speed and resistance of the exercise (Lloyd & Zacks, 1972; Cavagna & Kanenko, 1977). Similar efficiency measurements were calculated for performing successive deep knee bends, with a variable interval of time between the eccentric and concentric phases of the movement (Thys et al, 1972; Asmussen & Bonde-Petersen, 1974). These studies showed that the SSC

knee bends (with no time interval) were more efficient (26% to 41%) than the non-SSC knee bends (19% to 26%). Thys et al. (1975) also studied mechanical efficiency in rebound jumps of smaller amplitude. The efficiency values were found to be in excess of 50%, suggesting that movement amplitude affects the enhancement of mechanical efficiency by SSCs.

The results of these studies indicate that the marked performance enhancement observed in many SSC activities is dependent upon a variety of factors, including the type of task, the range of motion, the speed of contraction, and the coupling time between the stretch and shortening phases (Aura & Komi, 1987).

1.3 Explanations for SSC Enhancement

In an attempt to account for these observations, a variety of explanations for SSC enhancement have been proposed over the past few decades. It seems reasonable to consider each of these explanations to be, in part, true. However the limit of their influences remains unclear, as do the circumstances which are most favourable for exploiting them. The following sections briefly review these theories.

1.3.1 Recovery of Elastic Energy

In 1930, Fenn stated that muscle stiffness increases with the extent of muscle contraction and suggested that a muscle must be contracted in order to behave elastically. Hill (1950) showed that the SEC, a passive elastic element

linked in series with the muscle's contractile component, can accumulate elastic energy for future utilization.

In Cavagna's (1965) experiments on isolated frog muscle, the amount of positive work performed by a previously stretched muscle was found to be as much as twice that of the muscle contracted from rest. Since the neural drive, the length and the contraction velocity of the muscles could be carefully controlled, the results of these studies led the author to conclude that the extra work was being performed by strain energy, stored in the SEC during the active stretch. Based on the support of these findings, the enhanced performance observed in SSC activities was also believed to be due to the utilization of strain energy stored in the SEC. Cavagna explained the efficiency of walking, running and jumping as being due to this "elastic bounce" of the body. The apparent discrepancies between the mechanical efficiencies of running and jumping tasks compared to that of cycling, was explained as being due to the more suitable mechanism (SSC) for storing and recovering strain energy from the SEC in the running and jumping tasks.

In support of Cavagna's findings, a vast number of studies have attributed the majority of any observable SSC enhancement to elastic energy recovery (Komi & Bosco, 1978; Bosco et al., 1982; Shorten, 1987). However other SSC

influences, which can potentially affect movement performance, must also be considered.

1.3.2 Neural Potentiation

In the intact human system, neural connections to the muscle influence the mechanical outcome of muscular contractions. Because muscle stiffness increases with muscle activation, Cavagna (1977) proposed that the potential influence of a SSC should also increase with muscle activation. In addition, Bosco & Komi (1979) attributed part of the SSC influence on the enhancement of human movement performance, to neural potentiation caused by spinal and possibly cortical reflexes. They observed increased integrated electromyographic signals (IEMG) from the leg extensors during the concentric phase of vertical jumps performed with (vs. without) a counter-movement. However, the inconsistency of their findings led the authors to conclude that the relative contributions of neural and mechanical influences vary between subjects, as well as between tasks. These authors also warned that inhibitory reflexes could potentially play a detrimental role in movement performance outcome.

1.3.1 The INWASTE Theory

In 1984, Van Ingen Schenau published a rather controversial paper regarding SSC enhancement. He proposed that the amount of elastic energy which can be stored in, and

recovered from the SEC is small and can not sufficiently explain SSC enhancement in human movement. An alternative view of SSC enhancement was offered based on data from thermochemical experiments. This view suggested that an initial number of cross-bridges must do work in order to take up the "slack" of a muscle. The term INWASTE was coined to refer to this initial wastage of cross-bridges. It was suggested that in eccentric contractions, cross-bridges can attach without breaking down ATP. Because the amount of INWASTE is then minimal when a muscle is actively stretched prior to shortening, muscles undergoing a SSC can generate more force (or the same force at a lower metabolic cost) than muscles contracting from rest. With regard to complex multi-joint movements such as jumping, Van Ingen Schenau suggested that the muscle force at the onset of the concentric phase is greater in SSC movements because the counter-movement must be actively decelerated. This greater initial force would reduce or prevent the rise-time of muscle force and could account for much of the observed differences in performance.

1.3.4 Exploitation of Muscle Mechanics

In response to Van Ingen Schenau's INWASTE theory, Hof and Van den Berg (1986) presented quantitative evidence to show that more than adequate amounts of elastic energy can be stored in the SEC to be able to account for SSC enhancement in running. The differences between their calculations and Van

Ingen Schenau's lay principally in their estimates of SEC length. Hof and Van den Berg's distinction between internal (SEC and CC) and external (whole muscle) length changes led to considerably larger estimates of elastic energy storage.

Recent studies have provided more evidence to suggest that the SSC enhancement is at least partially due to a more optimal interaction between the neural drive to a muscle and the mechanics of muscular contraction. Thomson and Chapman (1988) demonstrated the advantages of the SSC in forearm supination tasks, remarking that the CC is permitted to work on a more effective portion of the force-velocity curve. Similarly, Hof (1990) used a theoretical Hill-based model of the plantar flexor muscles to demonstrate that SEC compliance could allow the CC to operate over more optimal ranges of the force-velocity and length-tension relations of muscle, during locomotion.

Dowling (1992) used a computer simulation to illustrate that movement velocity can be enhanced with a counter-movement in a musculoskeletal model which allows for no elastic recovery and no neural potentiation. In addition to reducing force rise-time, the initial stretching force was able to alter the length of the CC and SEC in such a way as to provide a preferable pattern of force generation. The associated muscle moments produced joint angular acceleration

patterns which generated higher angular velocities at given joint angles.

1.4 Hill-Based Muscle Models

A sound understanding of muscle function is fundamental to studying the complexities of human movement. Mathematical muscle models provide a means of simplifying a complex control system into a number of tractable mathematical equations (Zahalak, 1990). The complexity of these models depends largely on their purpose and on their scope. The purpose may be to accurately describe the intricacies of muscle function or simply to accurately estimate a particular parameter of muscle behaviour. The scope of the model's applications may be limited to specific muscles, specific actions or other specific circumstances. Keeping in mind the model's purpose and scope, a compromise must inevitably be made between a model's accuracy and its simplicity (Winters & Stark, 1987).

A wide assortment of muscle models have been developed by biomechanics researchers in an attempt to describe or predict muscle function. Many of these models are at least partially based on the classic work of A.V. Hill (1970). Hill showed that much of the macroscopic behaviour of muscle can be modelled by a contractile component (CC) linked in series with an elastic component (SEC) and in parallel with a visco-elastic component (PEC). Although the exact relationships are

not fully understood, it is generally agreed that the force
generated by the CC is a function of its activation, its
length and its contraction velocity (Winters, 1990). The
length and velocity (i.e. rate of change in length) of the CC
are in turn affected by the compliance of the SEC (Hof, 1990).

The relationships between the force generating
capacity of muscle and CC length and velocity have been
studied extensively both in vivo and in vitro. The compliance
of the SEC and PEC have also been modelled by numerous
researchers (for review see Ettema & Huijing, 1990). Lastly,
the relationship between EMG and muscle force has also
received considerable attention over the last few decades (for
review see Bigland-Ritchie, 1981). Previous modelling efforts
have used various combinations of various forms of these
elements in an attempt to estimate the force or torque
production of individual muscles or muscle groups (for review
see Winters, 1990).

Hof and Van den Berg (1981a,b) developed a model which
used EMG and kinematic measurements to estimate plantar
flexion moments during static and dynamic contractions of the
triceps surae muscles. The accuracy of the model was
relatively high (less than 20% error), considering the number
of simplifying assumptions that were involved. Similar models
have been developed for predicting individual muscle forces at
the human elbow (Dowling, 1987). Although more detailed

models do exist, it is generally accepted that Hill-based models offer a reasonably good compromise between model accuracy and complexity (Zahalak, 1990).

In summary, Hill-based models offer a useful tool for investigating human movement phenomena which either can not be directly observed, or can not be satisfactorily measured. In the previous section, four possible causes or contributors to the cause for SSC enhancement of performance were reviewed. At present, the relative importance of each is unknown in human movement. The use of a Hill-based muscle model allows each component's effect on movement performance to be partitioned out of the net effect that has been measured. It may be possible therefore, to use an EMG driven Hill-based model to answer the question of how much of an effect does elastic recovery, neural potentiation, INWASTE, or exploitation of muscle mechanics have on performance enhancement due to a SSC.

1.5 Purpose and Rationale for the Study

The main objective of this study was to accurately assess the significance of elastic recovery in a SSC elbow flexion task. The ability to do so could (1) improve our understanding of elastic recovery and stretch-shortening cycles, (2) help to identify implications of SSC use in movement control strategies and (3) improve current muscle models.

It is quite difficult to assess the magnitude or the significance of any individual SSC effect, such as the recovery of strain energy from the SEC, without the use of a muscle model which is able to account for the effects of other SSC phenomena. This problem is due to the virtually countless interactions which exist between the influences of the various neural and mechanical phenomena associated with SSCs. To begin with, the relationship between a muscle's force, its activation, its length and its rate of change of length is very non-linear and exceptionally complex. In addition, SSC movements may differ from non-SSC movements in many aspects of this complex relationship.

Consequently, the first aim of this study was to develop a mathematical Hill-based model of the human elbow joint, which was able to account for neural activation and internal muscle mechanics, in order to predict mechanical performance in non-SSC contractions. Because this model would have no ability to model the storage and utilization of elastic energy, it's estimation errors in specific SSC movements could be used to assess the magnitude and significance of elastic recovery in these movements.

1.6 Limitations and Assumptions of the Study

For the purposes of this study the validity of the model was evaluated by its ability to accurately estimate muscle function in non-SSC, concentric and isometric elbow

flexion contractions. It was the approach of this study that if the model was proven to be accurate through a fairly wide range of contractile conditions, it became reasonable to consider the model and its elements to be valid within the limits of those conditions. Thus, the specificity of the model's applications permitted a sacrifice of model universality in exchange for more accurate estimations.

Lastly, it was assumed that the only significant SSC phenomenon which could not be accounted for by the model was the recovery of elastic energy from the SEC. It was therefore also assumed that any underestimation of mechanical performance in SSC movements could be attributed to elastic recovery in those movements.

2.0 METHODS & PROCEDURES

A Hill-based model of the elbow joint was developed to estimate the torque and angular impulse generated by 8 subjects throughout a variety of elbow flexion contractions. The estimated impulse values were compared to measured values in order to assess and correct weaknesses in the model. The model did not include an element to account for storage or recovery of elastic energy. The significance of elastic recovery in SSC contractions was measured by inaccuracies of the model's estimates in those contractions.

2.1 The Model

The model used in this study was for the most part adapted from the elbow model of Dowling (1987). The elbow was regarded as a pure hinge joint with a fixed centre of rotation and a single degree of freedom (flexion/extension). Input information consisted of instantaneous measures of elbow joint angle and surface EMG from the elbow flexors and extensors. This input information was used by the model to estimate instantaneous net elbow moments. Figure 1 is a schematic diagram of the various input and output parameters of the model.

The net moment generated by the subject was calculated as the sum of an elbow flexor moment, an elbow extensor moment

16

17

INPUT   OUTPUT

JOINT ANGLE
                      MODEL   NET JOINT
EMG   MOMENT
(BIC/TRI)

Figure 1.   Schematic diagram of model input and output
parameters.

and a passive elbow moment. The flexor and extensor moments
were equal to the product of the force generated by the
functional muscle group and its instantaneous moment arm
length.   The forces generated by the two representational
muscles were the product of non-linear functions of muscle
activation (Afac), CC length (Lfac) and CC velocity (Vfac)
which are described in following sections.

2.1.1 Anatomical Model

        The moment arm length data were modified from the
equations of Dowling (1987), which were developed from the
data of Amis et al. (1979). The extensor moment arms were
chosen as those of the triceps brachii. Figure 2 illustrates
the moment arm data as a function of joint angle for the four
major muscles crossing the elbow.   A joint angle of 180
degrees was defined as full elbow extension.   The flexor
moment arms were calculated as a weighted average of those of
the biceps brachii, brachialis and brachioradialis muscles.

<u>Figure 2</u>. Muscle moment arm length as a function of elbow angle.

The relative torque contribution of each of these muscles was unknown and will most likely vary between subjects (Dul et al., 1984). Also, the moment arm data were deemed to be the weakest element of Dowling's (1987) elbow model. For these reasons, the relative weighting assigned to each of the three elbow flexor moment arm equations was determined by an optimization procedure described in more detail in section 2.4. Thus, the moment arm of the equivalent flexor muscle was

allowed to vary within the ranges depicted by the shaded area in Figure 2.

2.1.2 Activation-Force

Smoothed rectified surface EMG from the biceps brachii muscle was considered to represent the activation level of all functional elbow flexors. Similarly, EMG from the triceps brachii muscle was considered to represent the activation level of all functional elbow extensors. These assumptions are based on the work of Bouisset et al. (1977) and others (LeBozec et al., 1980) who have shown that these muscle groups behave as electrical equivalents when constrained to a single degree of freedom (flexion/extension). The relationship between activation and force generating capacity of the muscles is described by the following equation.

$$\text{(1)} \qquad Afac = A \times EMG^n$$

where: Afac = Muscle force based on muscle activation (N).
         A = Gain factor determined by optimization.
       EMG = Linear enveloped surface EMG (mV).
         n = Exponent factor determined by optimization.

The values of parameters A and n for each muscle group were determined by a best fit optimization procedure, which is described in more detail in section 2.4. The value of n was allowed to range between 0.4 and 1 based on previous studies (Milner-Brown & Stein, 1973; Chapman & Calvert, 1979) which suggest that the relationship between muscle force and EMG is

variably non-linear, with EMG amplitude tending to increase at a greater rate than force.

2.1.3 Length-Tension

The relationship between the force generating capacity of the muscles and the length of the muscle's contractile component (CC) was modelled as a bell-shaped function based on the work of Ismail and Ranatunga (1978). The function (Lfac) is described by the following equation and is illustrated in Figure 3.

$$
\textbf{(2)} \qquad Lfac = e^{\ln(.5) \times \frac{(Lcc - Lo)^2}{Lh^2}}
$$

where: Lfac = Length factor (0 - 1).
        Lcc = Length of the CC.
        Lo   = Optimal CC length for force generation.
        Lho = CC length away from Lo at which the force generating capacity is half of maximum when Sk=0.
        Lh   = Lho x Sk (if (Lcc-Lo)/Sk > 0)
               = Lho (if (Lcc-Lo)/Sk < or = 0)
        Sk   = Skew of the function (-4 to 4)

The values of parameters Lo, Lho and Sk for each muscle group were determined by a best fit optimization procedure described in a later section. The length of the CC was calculated as the difference between the length of the whole muscle and the length of the SEC. Whole muscle lengths were determined using a method adapted from Frigo and Pedotti (1978). This method defines the change in whole muscle length as the integral of the muscle's moment arm with respect to joint angle. This calculated length change was added to a

Figure 3. Length factor describing the force generating capacity of the muscle as a function of CC length.

constant length value, which had been previously determined for selected joint angles. The whole muscle lengths, calculated from the range of possible moment arm data, are plotted against elbow joint angle in Figure 4. The area between the biceps length (BIC) and brachialis length (BRA) depicts the range of possible lengths of the model's flexor muscle.

2.1.4 Series Elasticity

As stated previously, CC lengths were calculated by subtracting the instantaneous SEC length from the

Figure 4. Whole muscle length as a function of elbow angle.

instantaneous whole muscle length. The length of the SEC was

determined using the following equation.

(3) $Lsec = \dfrac{Lo}{100} \times SECm - (1 - \dfrac{Psec}{Po} + (SECm - 1) \times (1 - \dfrac{Psec}{Po})^{3})$

where: Lsec = Length of the SEC (% of Lo)
         SECm = Maximum length of the SEC (% of Lo)
         Psec = Tension across the SEC (CC force)
           Lo = Optimum isometric whole muscle length (m)
           Po = Optimum isometric force at Lo (N)

This relationship, which was adapted from Bahler (1978), is

illustrated in Figure 5. The value of SECm was determined by

a best-fit optimization procedure described in section 2.4.

Figure 5. SEC length as a function of CC force.

Based on the review paper by Close (1972), this maximum SEC stretch parameter was allowed to vary between 3 and 8 percent of the optimal whole muscle length.

2.1.5 Force-Velocity

The relationship between the force generating capacity of the muscles and the CC velocity were modelled as hyperbolic functions based on the force-velocity relationship studies of Faulkner et al. (1980). The function (Vfac) is described by the following equation and is illustrated in Figure 6. This figure illustrates the Vfac function for various levels of muscle activation and selected values of Vmax and Vh.

$$\textbf{(4)} \qquad Vfac = \left(\frac{a}{b + Vcc}\right) - k$$

$$\text{where:} \qquad k = \frac{-Vh}{2\left(Vh - \dfrac{Vm}{2}\right)}$$

$$b = Vm \times k$$

$$a = b(k + 1)$$

Vfac = CC Velocity factor (0 - 1.4).
Vcc = Rate of change of CC length.
Vm = CC velocity at which the muscle can
     generate zero force.
Vh = CC velocity at which the muscle can
     generate 50% of isometric force.

The instantaneous values of CC velocity were computed from the CC length data via a second-order central finite differences algorithm. Based on the elbow model of Dowling (1987), the parameter Vm was modelled to vary as a function of muscle activation. This element of the model is based on the assumption that the maximum shortening velocity of the CC increases as the activation of the muscle increases. This is presumably due to the recruitment of a greater proportion of fast twitch motor units at higher activation levels (Henneman, 1965). The following equation describes this function.

$$\textbf{(5)} \qquad Vm = Vmin + Vmax \times AS$$

where: Vm = CC velocity at which the muscle can generate
              zero force. (Lo/s)
        Vmax = CC velocity at which the muscle can generate
              zero force when 100% active. (Lo/s)
        Vmin = 1 Lo/s
          AS = Activation level of the muscle (% of max).

Figure 6. Velocity factor describing the force generating capacity of the muscle as a function of CC velocity.

2.1.6 Passive Visco-Elasticity

The following equations were adapted from Hayes and Hatze (1977) to describe the stiffness and viscosity of all the passive tissues crossing the elbow.

(6) $Pmom = PECg \times (S + V)$

(7) $$S = 0.036(\theta-60) - 1.8$$

(8) $$V = (0.545 - 0.526\theta - 0.165\theta^2)\,\omega$$

where: Pmom = Passive visco-elastic moment (N·m)
PECg = Gain value determined by optimization
S = Passive stiffness moment (N·m)
V = Passive viscosity moment (N·m)
θ = Elbow angle (degrees)
ω = Elbow angular velocity (rad/s)

The value of PECg was determined via the optimization procedure described in section 2.4. This value was allowed to vary between .5 and 1.5 in order to account for potential differences between subjects.

2.2 Procedures

The following sections describe in detail the methods employed to acquire the data for this study.

2.2.1 Subjects and Equipment

Eight healthy male subjects of average height (184 ± 3.9 cm), weight (79 ± 10.4 kg) and strength (64 ± 8.1 N·m isometric MVC torque at 120 deg elbow angle) were used for this study. After giving their informed consent to participate in the study, the following anthropometric data were obtained for each subject: height, weight and length of forearm (from medial epicondyle to ulnar styloid).

The following equipment and materials were used for the purposes of data collection. A modified Cybex II (Lumex) isokinetic dynamometer was used to isolate the desired

movement and to provide a quick release mechanism. A torque transducer (Lebow model #1253-117; 0-500 N·m range) and amplifier were used to measure the torque generated at the elbow. A load cell (Sensotec model #PEP; 0-1000 N range) and amplifier were used to measure the sharing of the load by a physical support. An electro-goniometer (0.3 deg resolution) and amplifier were used to monitor the elbow angle. Surface EMG recording electrodes (3M) and amplifiers (CMRR>90 dB; input impedance 100 MΩ) were used to record muscle activity. All data was acquired and digitally converted using a 12-bit A/D data acquisition unit (WATSCOPE, Northern Digital) and a microcomputer (Amdek 80286). A CRT oscilloscope (Dynascan model #2520) was used to display the joint angle signal to the subject during the experiment. The experimental set-up is illustrated in Appendix B and is explained in more detail in the following sections.

2.2.2 Cybex Modifications

The Cybex II dynamometer was modified by fixing a chain wheel to the axle of the dynamometer to allow for external torque application. In addition, a torque transducer was mounted between this chain wheel and the dynamometer crank arm. Thus, the torque transducer was able to measure the sum of the torques applied distal to the transducer.

The resistance to movement could be manipulated in three ways. First, an isotonic resistance could be applied by

hanging weights from a custom designed pulley system connected in series with the chain wheel. Secondly, an isokinetic resistance could be applied by an internal electromagnet, which could limit the maximum angular velocity to selected values (ranging from isometric to 300 deg/s). Thirdly, a micro-switch was added to allow for a controlled "quick-release" from an isometric electromagnetic resistance to any other selected isokinetic resistance. Finally, the crank arm was modified with a padded metal plate in order to support the weight of the subject's forearm between experimental trials.

2.2.3 Electromyography

Each subject's right arm was shaved and cleaned for electrode placement. Bipolar Ag/AgCl surface EMG recording electrodes (10 mm diameter) were placed approximately 3 cm apart (centre to centre) along the length of the bellies of the long head of the biceps brachii and the middle head of the triceps brachii muscles. A common reference electrode was placed over the anterior aspect of the forearm. The electrical impedance following skin preparation was always less than 8 kΩ.

The recorded signal was pre-amplified (100X) at the electrode location before being variably amplified, band-pass filtered (10-500 Hz), A/D converted (1000 Hz) and stored on disk. The resulting signal was full-wave rectified and

filtered via a second-order critically damped, low-pass digital filter (3 Hz cutoff).

2.2.4 Kinematics

The centre of rotation of the electro-goniometer (ELGON) was placed over the medial epicondyle of the subject's right arm. The arms of the ELGON were aligned with the long axes of the humerus and ulna and secured to the subject's arm and forearm with adhesive tape. The joint angle signal was amplified, A/D converted (200 Hz) and stored on disk. The ELGON signal was also displayed on an oscilloscope in view of the subject, so that they were able to monitor their elbow angle during the course of the experiment. The stored ELGON signal was smoothed using a dual-pass, second order, Butterworth low-pass digital filter (10 Hz cutoff). A second order central finite differences algorithm was used to obtain angular velocities and accelerations.

2.2.5 Torque and Angular Impulse

The signal obtained from the torque transducer was amplified, A/D converted (200 Hz) and stored on disk for further analysis. The torque measured by the transducer (Tt) was the sum of the following: (1) the torque applied by the subject (Ts), (2) the torque due to the force of gravity acting on the arm and crank apparatus (Tg), (3) inertial torques opposing the angular acceleration of the arm and crank apparatus (Ti), (4) torque applied by the physical rest (Tr).

The following equations describe how the torque applied by the subject was calculated.

(8)
$$Ts = Tt + Tg + Ti - Tr$$

(9)
$$Tg = m_a \times g \times cga \times \cos(AA)$$

(10)
$$Ti = \alpha \times Ia$$

(11)
$$Tr = Fr \times Lr$$

where: g = acceleration due to gravity
 m_a = mass of arm assembly and forearm
 cga = centre of gravity of arm assembly and forearm
 AA = angle of arm assembly relative to horizontal
 α = joint angular acceleration
 Ia = moment of inertia of the arm assembly and forearm
 Fr = reaction force applied by the physical rest
 Lr = distance from axis of rotation to mechanical rest

The moment of inertia of the forearm was calculated based on the anthropometric tables of Winter (1979). The reaction forces applied by the physical rest to the arm assembly were measured by a load cell mounted on the arm assembly itself. The signal from the load cell was amplified, A/D converted (200 Hz) and stored on disk. The absolute angle of the arm assembly was determined from the joint angle measurements based on a calibration performed with the forearm in a horizontal position. The angular impulse generated by the subject was calculated as the first integral with respect to time, of the torque applied by the subject (Ts).

2.3 Experimental Protocol

The subject was seated with their right arm resting on the modified arm assembly. The subject's lateral epicondyle was aligned with the axle of the modified Cybex arm assembly before being secured to the crank arm with Velcro straps. The subject was also secured to the chair at the waist and across the upper chest and shoulders in order to minimize any movements other than elbow flexion or extension. The subject then performed a series of each of the following three types of contractions: stretch-shortening (SS), quick-release (QR), and concentric (CO).

2.3.1 Stretch Shortening Contractions

The subject's arm was locked in a vertical position (corresponding to approximately 70 degrees of elbow extension) from which position the resistance was released. After release, a 20 N·m external torque, in addition to the force of gravity acting on the arm assembly, tended to extend the elbow. The subject was instructed to try to resist extension and then maximally flex the elbow such that the elbow would extend to a target angle of approximately 120 degrees and then flex back to its initial position in as short a time as possible. The subject was able to monitor their elbow angle on the oscilloscope throughout the movement. The subject was instructed to begin resisting extension only at the latest possible instant, keeping in mind that they needed to achieve

maximal extension at the target angle. A series of these trials were performed until at least four trials met the following criteria: (1) the maximal elbow angle was within two degrees of the target angle, (2) the subject felt that their effort was maximal, (3) the movement was limited to elbow flexion and extension. Adequate rest was provided between trials in order to prevent muscle fatigue. The maximal angular velocity was set at 300 deg/s, thus there was no isokinetic resistance because of the low velocities at which the subjects were able to move against the isotonic resistance.

2.3.2 Quick Release Contractions

A target angle was determined by the mean maximal angle of the SS contractions. The subject's arm was locked in that position prior to the release of the isometric resistance. The subject was then asked to perform an isometric maximal voluntary contraction (MVC) of the elbow flexors for approximately 1 to 2 seconds, after which the isometric electromagnetic resistance was released. The subject was instructed to continue to maximally contract their elbow flexors after release, until full elbow flexion was achieved. The maximal angular velocity was set at 300 deg/s and the isotonic resistance at 20 N·m, as for the SS contractions. The subject was asked to perform four of these

contractions. Again, adequate rest was allowed in order to prevent muscle fatigue.

2.3.3 Concentric Contractions

The subject's arm was supported by a physical rest, in the target position described in the previous section. The subject was then asked to perform a concentric MVC of the elbow flexors until a position of full flexion was achieved. The isometric resistance was not used in these contractions. The maximal angular velocity was set at 300 deg/s and the isotonic resistance at 20 N·m as for the SS and QR contractions. The subjects performed four of these contractions separated in time by an adequate rest interval.

2.3.4 Calibration Trials

In addition to the experimental contractions described above, the subjects also performed the contractions listed in Table 1 to provide data for the purpose of determining the model's parameter values. These calibration data covered a wide range of contractile conditions, with the exclusion of SSC situations.

In Table 1, a ramp effort is defined as a slow increase from rest to maximum effort over a period of 3 to 4 seconds. A coactive effort is defined as a voluntary activation of both the elbow flexors and extensors throughout the movement; and a submax effort is defined as what the subject perceived to be a 50% effort. In addition to these

Table I. Description of the calibration trials.

Initial Angle	Flex/Ext	Maximum Velocity	Isotonic Resistance	Effort
120 deg	Flex	Isometric	0 N.m	Ramp
120 deg	Ext	Isometric	0 N.m	Ramp
90 deg	Flex	Isometric	0 N.m	Ramp
90 deg	Ext	Isometric	0 N.m	Ramp
160 deg	Flex	300 deg/s	0 N.m	Max
160 deg	Flex	300 deg/s	0 N.m	Submax
160 deg	Flex	300 deg/s	0 N.m	CoAct
160 deg	Flex	30 deg/s	20 N.m	Max
160 deg	Flex	30 deg/s	20 N.m	Submax
160 deg	Flex	120 deg/s	20 N.m	Max
160 deg	Flex	120 deg/s	20 N.m	Submax
160 deg	Flex	300 deg/s	40 N.m	Max
160 deg	Flex	300 deg/s	40 N.m	Submax

trials, those experimental trials not used in the statistical analysis (because they didn't meet the selection criteria) were also used in the calibration process.

2.4 Model Calibration and Optimization

The calibration of the model for each subject required the estimation of values for 20 model parameters (the following 8 for each muscle group: A, n, Lo, Lho, Sk, SECm, Vh, Vmax; as well as rBIC, rBRA, rBRD and PECg). The role of each of these parameters in the model is illustrated in Figure 7. The value of these parameters were calculated by a best fit optimization procedure similar to that described by Hatze (1981). The model was applied to a series of experimental data which spanned a wide range of contractile conditions. The estimated net angular impulses generated by the subject

Figure 7. Detailed schematic diagram illustrating the role of the muscle model's parameters.

were compared to the measured angular impulses using a least squares method to determine the model prediction error. This optimization procedure consisted of a systematic, step-wise modification of the parameter values with the aim of minimizing the model prediction error for the calibration data of each subject. The calibration trials were designed to include situations of moderate to high activation levels of

the elbow flexors and low to moderate activation levels of the elbow extensors through a wide range of joint angles and joint angular velocities. These trials were limited to concentric or isometric, non stretch-shortening situations and the optimal parameter values were limited to the ranges listed in Table 2. These ranges were based on previous investigations relating to each parameter as discussed in previous sections.

Table II. Upper and lower limits of model parameter values used by the optimization procedure.

Parameter	Flexor Limits	Extensor Limits
A	none	none
n	0.4 - 1.0	1.0
Lo	0.10 - 0.45 m	0.15 - 0.25 m
Lho	0.1 - 0.9 Lo	0.1 - 0.9 Lo
Sk	-4.0 - 4.0	-
Vmax	2.0 - 10 Lo/s	2.0 - 10 Lo/s
Vh	1 Lo/s - 0.5 Vm	1 Lo/s - 0.5 Vm
SECm	0.03 - 0.08 Lo	0.05 Lo
PECg	0.5 - 1.5	
rBIC	0 - 1.0	
rBRA	0 - 1.0	
rBRD	0 - 1.0	

2.5 Hypotheses and Statistical Analysis

The angular velocity and the angular impulse generated by the subject (over the first 100 ms of the concentric phase of the movements) were the variables selected to compare the performance of the different contractions. The first 100 ms was chosen since this has been reported as the time frame over which most elastic recovery occurs (Mungiole & Winters, 1991).

The estimation errors (RMS) of the angular impulse-time histories were used to assess the accuracy of the model.

A three factor (3 [contraction type] X 4 [trial order] X 2 [angular impulse measure]) analysis of variance (ANOVA) was used to assess the effects of these factors on the performance measures. It was hypothesized that the angular impulse and velocities generated in the SS condition would be significantly greater than those of the QR and CO conditions. It was also hypothesized that the accuracy of the model's estimates would be significantly poorer for the SS contractions than for either of the other two contraction types. The effect of trial order was expected to be insignificant.

3.0 RESULTS AND DISCUSSION

This chapter summarizes the results of the study as follows. First, the accuracy of the model is assessed with respect to estimating the performance of non-SSC movements. Secondly, representative data are used to illustrate performance differences between the three types of contractions (SS, QR, CO). Thirdly, the model's estimates are used to assess the effects of contraction type on model accuracy. Fourthly, differences in muscle activation patterns between the three contraction types are presented. Lastly, the results of these analyses are interpreted with respect to describing and explaining elastic recovery in SSC movements.

3.1 Accuracy of the Model

The methods used in this study relied heavily on the use of a model which could accurately predict movement performance in non-SSC, concentric contractions. Since the model was essentially developed to estimate instantaneous elbow torque, this parameter would seem to be the most appropriate for measuring model accuracy as well. However, it was judged that angular impulse (AI) estimates would be a preferable measure of model accuracy. This parameter is more sensitive to systematic errors in torque estimates. Because AI is the integral of torque with respect to time, systematic

errors in torque estimates would tend to accumulate over time in estimates of angular impulse. Thus, the least squares method used in the model's optimization tended to minimize systematic errors in joint torque estimates.

3.1.1 Goodness of Fit Measures

The instantaneous error of the model's angular impulse estimates was calculated for each sampled point in time from the concentric phase of all the non-SSC contractions performed by each subject. These goodness of fit results are summarized by a root mean squared (RMS) error and a percent RMS error value for each subject's data. The percent RMS error value was calculated as the ratio between the RMS error and the RMS value of the measured impulse. These data are presented in Table 3, along with the associated average, RMS and %RMS errors in elbow torque estimates.

Table III. Accuracy of the model's performance estimates in non-SSC contractions for each subject.

Subject #	AI Errors		Torque Errors		
	RMS (N·m·s)	%RMS (%)	Avg (N·m)	RMS (N·m)	%RMS (%)
1	1.54	26.2	-6.5	12.1	33.0
2	0.69	10.6	-2.5	6.0	16.0
3	0.46	8.4	0.8	5.9	15.2
4	0.86	15.4	-1.1	16.9	36.2
5	0.45	7.5	-2.2	5.4	16.8
6	0.27	6.2	-0.2	5.6	16.9
7	0.61	9.1	-3.1	10.5	28.6
8	1.17	18.6	2.5	10.9	30.6

From the error values listed in Table 3 it can be seen that the overall model error was always less than 26.2% for the non-SSC contractions of each subject. The corresponding errors in joint torque estimates ranged between 15 and 36 percent. The error of the torque and angular impulse estimates were calculated such that a negative error represents an overestimation, and a positive error represents an underestimation by the model. With the exception of subject #1 (-6.5 N$\cdot$m), the average error of the torque estimates was very close to zero for all subjects ($\pm$ 3 N.m). This suggests that there were no gross systematic errors in the model's estimates of joint torques and that the accuracy of the model was suitable for estimating the performance of non-SSC movements. Based on these findings, the accuracy of the model was then assessed in each of the three experimental conditions (SS, QR, CO). Prior to presenting the results of this analysis, data from a representative set of trials are presented to illustrate performance differences between the three experimental conditions.

3.2 Performance Differences

Figure 8 illustrates elbow joint angle as a function of time, for a representative set of trials performed by subject #5. The joint angular velocity, joint torque and angular impulse vs time curves associated with those same trials are illustrated in Figures 9, 10 and 11, respectively.

It can be seen from Figure 8 that the SS contractions typically covered a greater range of motion over the first 200 to 250 ms of the concentric phase than did the other contractions. This was the case for all subjects. This was also the time period during which the SS movements typically achieved their highest angular velocity (Fig. 9). It should be noted that because of small levels of noise in the velocity data, the onset of the concentric phase was defined as the time of the first velocity value above 0.2 rad/s.

The marked kinematic differences between contraction types were the result of differences in torque generation patterns. Figure 10 clearly illustrates these differences. In this particular series of contractions, the SS torque was maximal at the onset of the concentric phase and declined steadily as the movement progressed. The QR torque was also maximal at the onset of the concentric phase (but smaller than the SS maximal torque), after which it declined rapidly and then remained relatively constant as the movement progressed. The CO torque did not reach its maximum value until roughly 150 ms into the concentric phase, after which it remained relatively constant. The effects of these different patterns of torque generation on movement performance are illustrated nicely by the angular impulse curves of Figure 11. The early differences in torque production resulted in significant variations in the angular impulse generated over the first 100
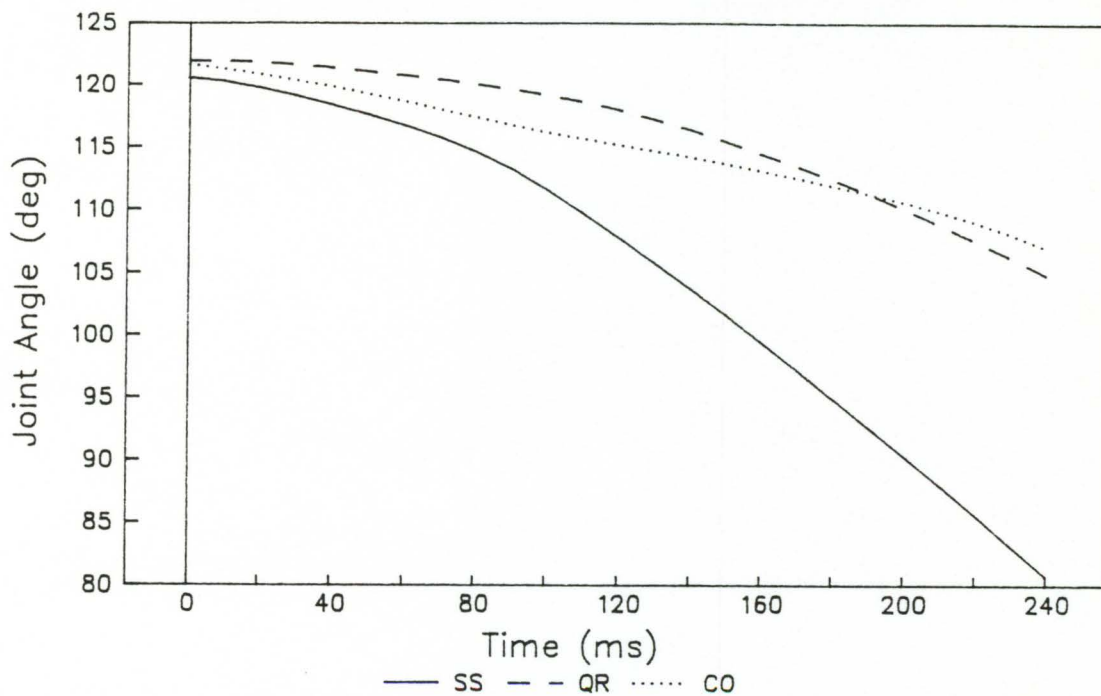

42

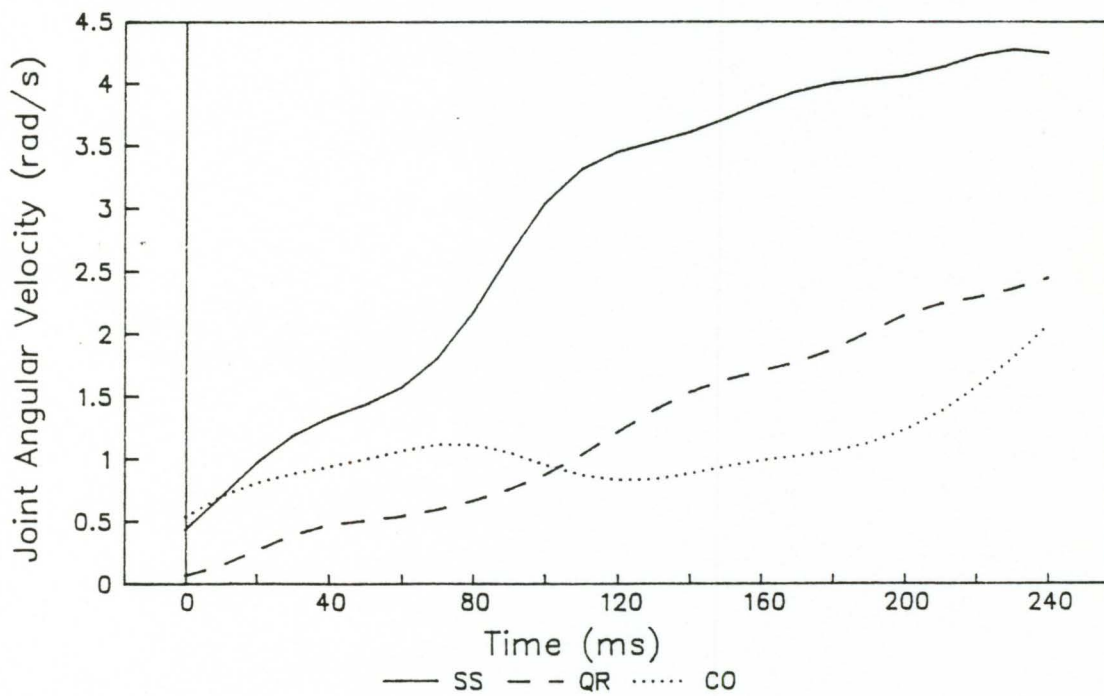Figure 8. Elbow joint angle vs time for representative SS, QR and CO contractions.

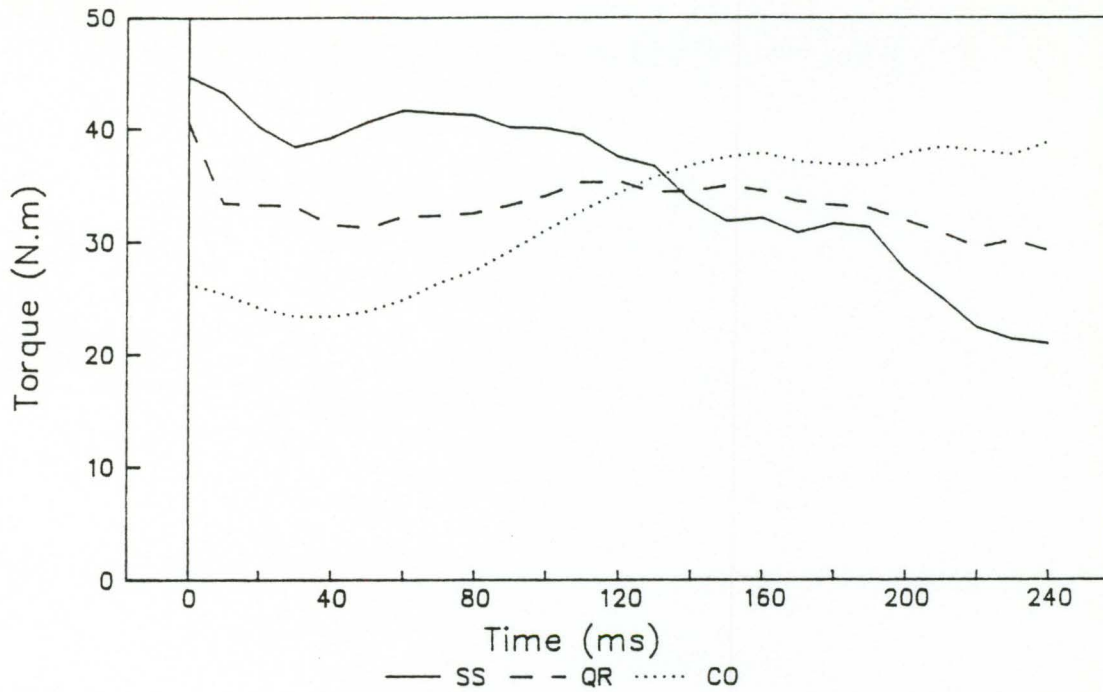Figure 9. Joint angular velocity vs time for representative SS, QR and CO contractions.

Figure 10. Elbow torque vs time for representative SS, QR and CO contractions.
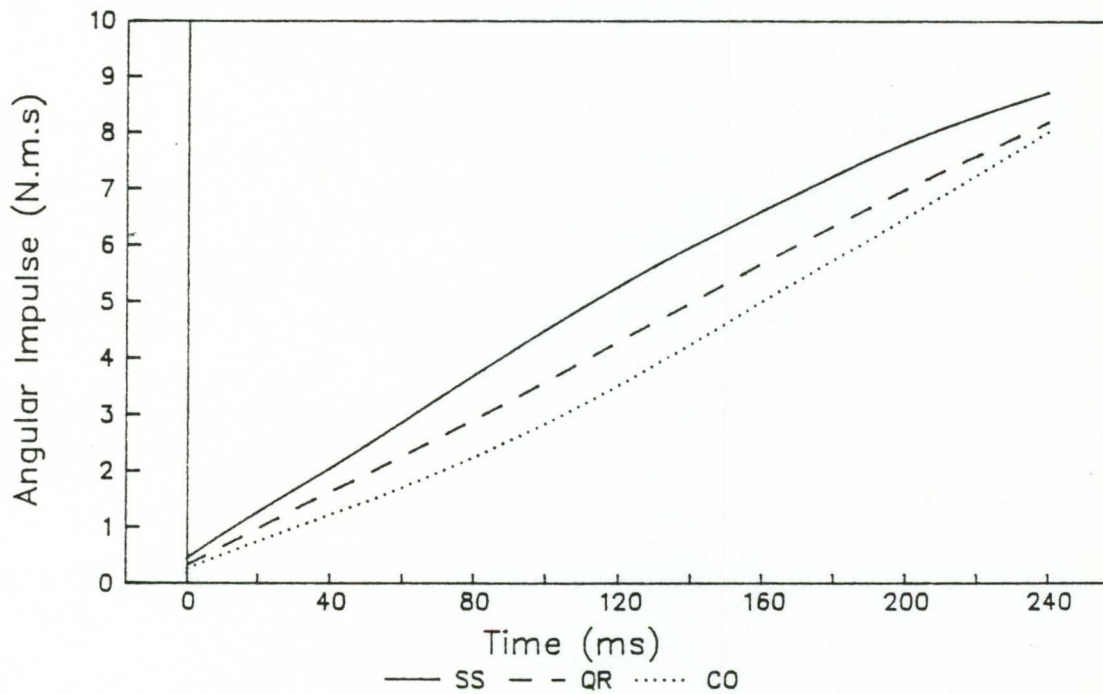

Figure 11. Angular impulse vs time for representative SS, QR and CO contractions.

to 120 ms of the three contractions. These differences in angular impulse tended to decrease after this time, as the torque patterns tended to reverse (Fig. 10). A statistical analysis was performed on the angular impulse data to assess the significance of the observed differences.

3.2.1 Angular Impulse

A 3-way (3 [contraction type] X 4 [trial order] X 2 [impulse measure]), repeated measures ANOVA enabled the assessement of both movement performance and model accuracy in the three experimental conditions. The dependent variable was the angular impulse generated by the subject over the first 100 ms of the concentric phase of the movement. This parameter is analogous to the average torque generated by the subject over that time period. A period of 100 ms was chosen because this was the time frame over which the majority of the performance differences were observed (Figs. 9 and 11). This time frame was also reported by Mungiole and Winters (1991) to be the period over which most elastic energy recovery occurs.

As was expected, trial order had no significant effects on the dependent measure. However, a significant interaction was observed between contraction type and impulse measure. Tukey HSD post-hoc tests were performed to determine the source of this interaction. Figure 12 illustrates the mean (± standard error) measured and estimated angular impulse values for the three contraction types.

Figure 12. Mean (± SE) measured and estimated angular impulse generated over the first 100 ms of the concentric phase of the three contraction types.

It can be seen from Figure 12, that the mean measured angular impulse was significantly greater (p>.001) in the SS contractions (4.94 N·m·s) than in the QR (3.91 N·m·s) or CO (3.99 N·m·s) contractions. These results indicate that the active pre-stretch of the SS contractions enhanced the performance of these contractions relative to both the trials starting from rest (CO) and those starting from an isometric pre-activation (QR). Furthermore, the estimated angular impulse was only significantly different from the measured angular impulse in the SS contractions. The mean estimated

angular impulse in the SS condition (4.07 N·m·s) was approximately 20 percent smaller than the measured value. This finding suggests that the model was unable to account for an important source of angular impulse which was available only in the SS contractions. The interpretation of the model's estimation errors will be discussed in more detail in sections 3.3 and 3.4.

3.2.2 Angular Velocity

Angular velocity is usually a more familiar measure of performance in ballistic type movements than angular impulse. For this reason, angular velocity was also compared across contraction types and performance measures (estimated vs measured). The angular velocity gained over the first 100 ms of the concentric phase of the movement was used as this measure. The estimated value of this parameter was calculated as the first integral (with respect to time) of the estimated net torque, divided by the moment of inertia of the forearm and arm assembly. The net torque was equal to the difference between the torque generated by the subject and the external resistance torque measured by the transducer.

Figure 13 illustrates the mean (± standard error) measured and estimated mean angular velocities for the three contraction types. As was observed from the angular impulse measures, a performance enhancement was evident in the SS trials. The mean measured angular velocity of 2.74 rad/s
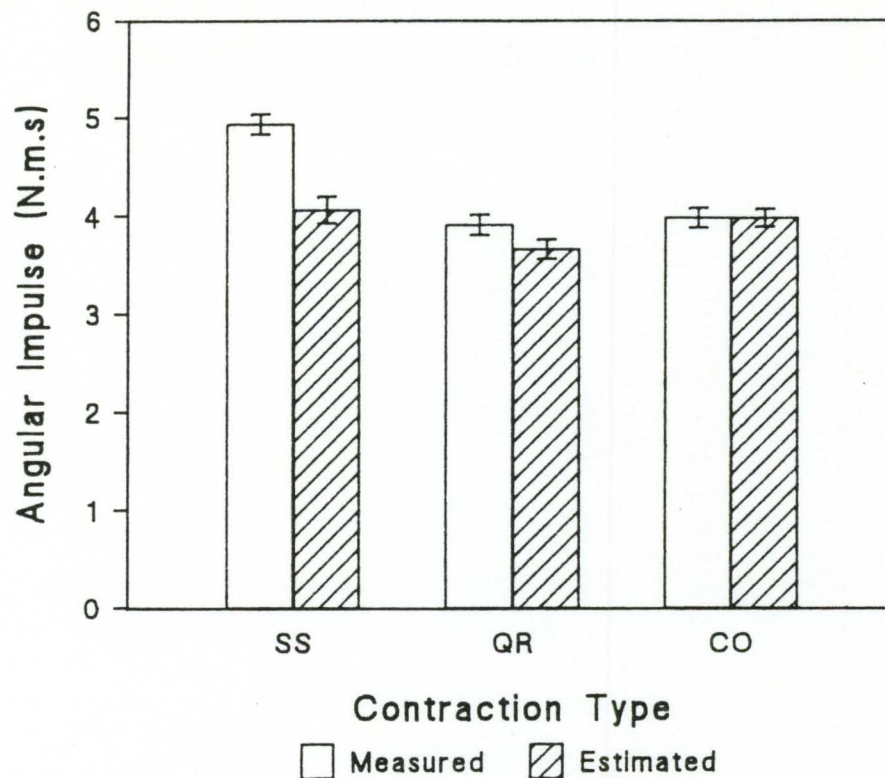
Figure 13. Mean (± SE) measured and estimated angular velocities generated over the first 100 ms of the concentric phase of the three contraction types.

obtained in the SS trials was notably greater than that obtained by either the QR trials (1.74 rad/s) or the CO trials (2.13 rad/s). Clearly however, the estimated velocities were inaccurate in both the SS and the QR contractions. The 20% underestimation of the SS angular impulse (mean torque) resulted in a mean estimated angular velocity (-1.67 rad/s) which was actually opposite in direction from the true movement's velocity (2.74 rad/s). This illustrates how small errors in torque estimates can be magnified and may accumulate, causing large errors in velocity or displacement

estimates. It was for this reason that angular impulse was selected as the primary performance measure for this study, rather than angular velocity. The following section discusses the characteristic pattern of the model's estimation errors observed in the SS condition.

3.3 Model Estimation Errors

As was stated in the previous section, the model significantly underestimated the angular impulse generated by the SS contractions. The errors in torque and angular impulse estimatations for the same series of trials presented in Figures 8-11, are illustrated in Figures 14 and 15 respectively. Figure 14 shows how the errors in SS torque estimates were typically very large at the onset of the concentric phase (in this case 50% of the true torque). These underestimation errors tended to diminish to the same level as the QR and CO errors by about 100 to 150 ms into the concentric phase. Similar error patterns were observed in the model's estimates for the SS contractions of all 8 subjects. Figure 15 illustrates how these systematic torque estimation errors caused large angular impulse estimation errors.

According to impulse-momentum theory, net angular impulse determines changes in angular velocity. For the purposes of this study, the net angular impulse was defined as the difference between the impulse generated by the subject and the resistance impulse. If the magnitude of the angular

<u>Figure 14</u>. Elbow torque estimation error vs time for
representative SS, QR and CO contractions by subject #5.

impulse errors (Fig. 15) are compared to those of the net

angular impulse (Fig. 16) it can be seen that in the SS

condition, these errors often surpass 100% of the true

signal's amplitude. These errors would be magnified even

further if one was to examine angular displacement estimates.

It is obvious from these examples, that estimates of the

kinematics of human movement are extremely sensitive to errors

in estimates of the kinetic variables from which they are

derived. Undoubtedly, a better understanding of SSC phenomena

would improve the accuracy of such estimates and is crucial to

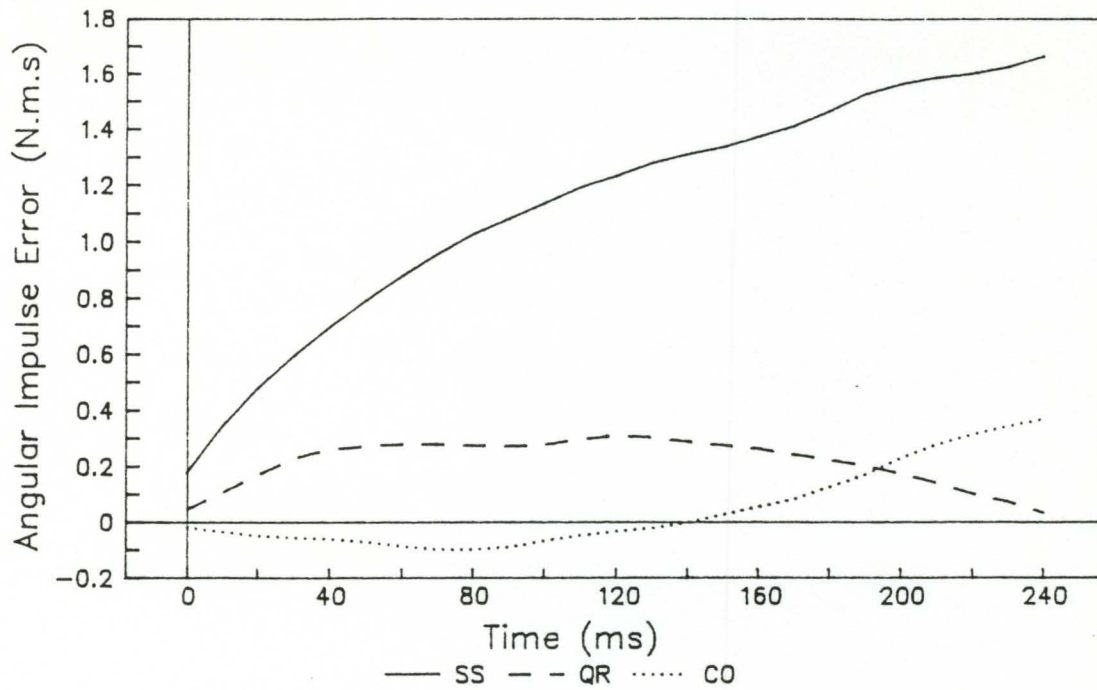the development of truly reliable models of muscle function.

Figure 15. Angular impulse estimation errors for representative SS, QR and CO contractions.

Figure 16. Net angular impulse vs. time for representative SS, QR and CO contractions.

3.4   Interpretation of Results

The results of this study can be summarized by the following two statements: (1) a performance enhancement was observed in the SS contractions, and (2) this enhanced performance was not fully accounted for by the muscle model. The following sections will first discuss the SSC influences which the model could presumably account for. These influences include muscle activation patterns and the exploitation of contractile component mechanics. Following this, the unexplained performance enhancement is interpreted, with respect to the potential influences of SSC phenomena which were not accounted for by the model. Particular consideration is given to the influence of elastic energy recovery.

3.4.1   Muscle Activation Patterns

An important feature of this study's design was the ability of the model to account for muscle activation differences during voluntary efforts. Past studies examining SSC enhancement have typically either used a stimulation protocol to control for activation (Cavagna et al., 1965), assumed maximal voluntary effort (Wilson et al., 1991), or measured muscle activity without being able to relate activation differences to performance differences (Bosco et al., 1982). Through the use of an EMG driven muscle model, not only can voluntary activation differences be measured, but

the effects of these differences on movement performance can also be assessed.

A second important feature of the model used in this study was it's ability to account for resistance generated by antagonist muscles. Co-contraction of antagonist muscles has been shown to vary between individuals and between tasks (Basmajian, 1985). By estimating the moments of force generated by the elbow extensors, the model was able to account for the influences of this factor on movement performance.

Figures 17 and 18 illustrate the activation levels of the triceps and biceps muscles respectively, as measured during a representative series of SS, QR and CO contractions performed by subject #5. As can be seen from Figure 17, the triceps activation was typically quite low (< 20%) and did not demonstrate systematic differences between contraction types. For these reasons, variation in triceps activation was not considered to be a major contributor to the performance differences observed between contraction types.

The flexor activation patterns of the three contraction types typically displayed some divergence over the first 50 to 100 ms (Fig. 18). The SS contractions showed the highest activation at the onset of the concentric phase and the CO contractions exhibited the lowest.
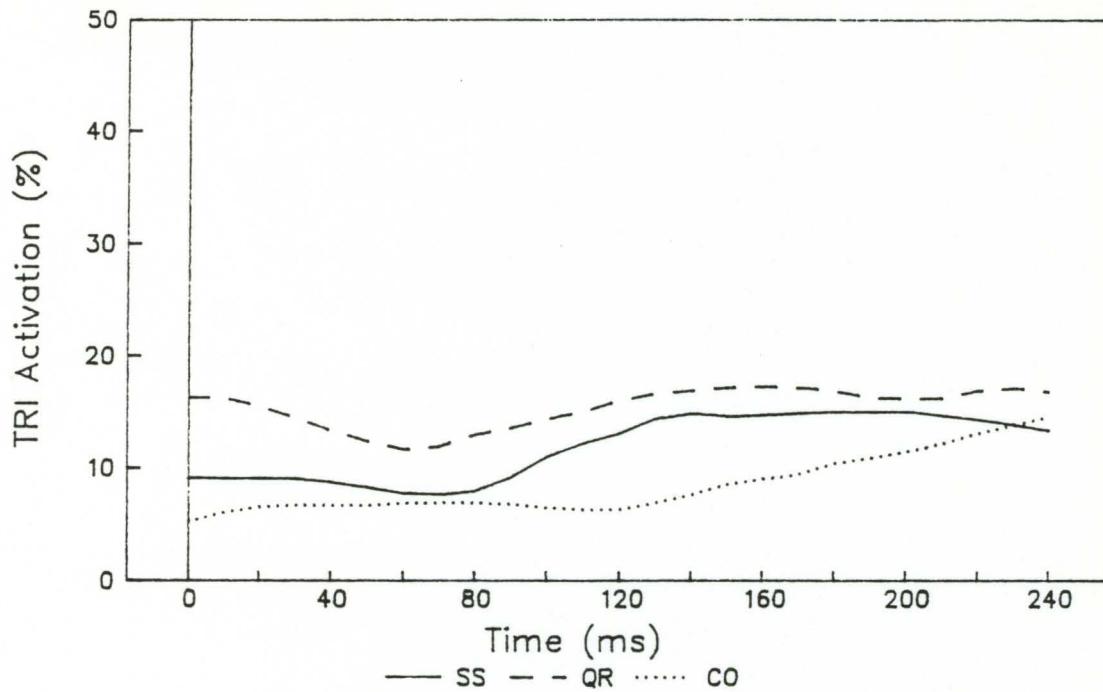
Figure 17. Activation level of the triceps brachii muscle measured during representative SS, QR and CO contractions.

Figure 18. Activation level of the biceps brachii muscle measured during representative SS, QR and CO contractions.

A two-factor ANOVA (3 [contraction type] X 4 [trial order]) revealed a significant main effect of contraction type on the average activation level of the biceps (measured over the first 100 ms of the concentric phase). The activation level of the SS contractions (75%) was significantly greater (p<.01) than in either the QR (65%) or the CO (63%) contractions. This difference may have been the result of neural potentiation associated with a stretch reflex induced by the counter-movement (Bosco et al., 1982). The QR contractions showed high initial activity which was sometimes followed by a distinctive decrease in activity, following the release of the isometric resistance. This decrease in activity may have been some form of protection against injury, possibly caused by uncertainty regarding the anticipated rapid change in resistance.

Since the CO contractions started from rest, they typically required a period of 50 to 100 ms to reach the same activation levels as those of the other conditions, and therefore showed a lower average activation level over this period. It should be noted however, that at the onset of the CO contractions, there was a sharing of the load between the subject and the arm support. This allowed the flexor muscles to attain a moderate level of activation prior to the first significant decrease in joint angle, which was used to define the start of the concentric phase. It should also be noted

that these characteristic patterns were not observed in all contractions and that a substantial amount of variability existed between subjects.

In spite of differences in muscle activation between the three contraction types, no significant differences in estimated angular impulse were observed. This suggests that either the effects of neural potentiation on performance were negligible, or that other factors tended to oppose these neural effects. For example, an increase in CC force caused by neural potentiation would tend to cause the CC to shorten at a faster rate, which in turn would tend to decrease the force generating capacity of the CC. The net effect of these interactions may be the production of identical muscle forces regardless of dissimilarities in muscle activation.

In summary, a neural potentiation was observed in the SS contractions. However based on the model's estimations, this neural potentiation, in conjunction with associated discrepancies in CC mechanics, caused no significant improvement in movement performance. The enhanced performance was therefore attributed to other SSC influences which were not accounted for by the model.

3.4.2 Explaining SSC Enhancement

Chapter 1 outlined four SSC phenomena capable of enhancing movement performance: series elastic recovery, neural potentiation, decreased INWASTE and exploitation of

muscle mechanics. Of these four phenomena, only INWASTE and series elastic recovery were not accounted for by the model. It can therefore be presumed that the unexplained SSC performance enhancement originated from either one or both of these sources.

The concept of INWASTE (Van Ingen Schenau, 1984) relies on knowledge concerning the thermodynamics of cross-bridge mechanics. A lack of reliable measurement techniques for such information has made it difficult to assess the influences of INWASTE on the behaviour of muscles. Thus, although the INWASTE explanation of SSC enhancement can not be entirely refuted, it has received very little empirical support since it was first proposed. On the other hand, the potential of muscle to store and recover elastic energy has been observed in numerous carefully controlled experiments (Shorten, 1987). In addition, although the QR contractions should theoretically have benefitted from a reduction in INWASTE, the model demonstrated no significant errors in predicting the performance of those contractions. For these reasons, it seems reasonable to attribute the bulk of the unexplained SSC performance enhancement to elastic energy recovery.

It could be argued that the SS contractions differed from the other contractions in certain aspects of activation, length or velocity, such that estimation errors caused by

flaws in the model's elements were biased towards the SS contractions. This possibility was explored by attempting to modify the model's functions to better fit the SS data while maintaining a high degree of accuracy in non-SSC contractions. Such modifications of the model were unable to improve the SS estimations by any substantial amount. Furthermore, the calibration trials used to determine the model's optimum parameter values exceeded the ranges of activation, joint angle, joint angular velocity and torque which were produced in the experimental trials. This suggests that the SS contractions likely did not surpass the scope of the model's validity with respect to those parameters. Lastly, the optimized parameter values of the model showed reasonable agreement between subjects. The ranges of these values are listed in Table 4. Because of the wide range of contractile conditions which were assessed, this agreement suggests that the model reflected some underlying principles of muscle function which were common to all subjects. It would therefore seem reasonable to assume that the SS contractions made use of phenomena which were not included in the model, rather than differing in their utilization of phenomena which were modelled.

3.4.3 Predicting SSC Enhancement

Based on the arguments presented in the previous section, a significant portion of SSC enhancement can be

Table IV.   Ranges of model parameter values determined by optimization (F=flexor, E=extensor).

Parameter		Minimum	Maximum	Mean
Lo	(F)	0.336 m	0.361 m	0.349 m
Lh	(F)	0.011 m	0.053 m	0.024 m
Sk	(F)	-4.0	4.0	-0.625
SECm	(F)	0.05 Lo	0.08 Lo	0.06 Lo
Vmax	(F)	3.0 Lo/s	9.0 Lo/s	5.34 Lo/s
Vho	(F)	0.26 Vm	0.36 Vm	0.33 Vm
n	(F)	0.40	0.60	0.45
A	(F)	5.67	12.1	9.13
Lo	(E)	0.324 m	0.450 m	0.388 m
Lh	(E)	0.011 m	0.100 m	0.056 m
Sk	(E)	0.0	0.0	0.0
SECm	(E)	0.05 Lo	0.05 Lo	0.05 Lo
Vmax	(E)	6.0 Lo/s	9.0 Lo/s	7.6 Lo/s
Vh	(E)	0.24 Vm	0.46 Vm	0.34 Vm
n	(E)	1.0	1.0	1.0
A	(E)	0.8	5.1	1.9
PECg		0.5	1.5	0.86
rBIC		0.00	0.40	0.20
rBRA		0.00	1.00	0.38
rBRD		0.00	1.00	0.42

confidently attributed to series elastic recovery. From a muscle modelling point of view, the next step would be to attempt to quantitatively predict SSC enhancement from observable measurements. The form of this predictive function would depend largely on the purpose and scope of the muscle model. For example, if the objective of a particular muscle model is to accurately predict individual muscle forces, then the extra force associated with a SSC would be the parameter of interest. This magnitude of the extra force might be best predicted by a combination of many parameters, such as stretch amplitude, stretch velocity, SEC tension, strain energy, rate

of change of strain energy, and possibly many others. These types of predictions were beyond the scope of the present study. The SSC contractions employed in this study were limited to a very narrow range of contractile conditions (as opposed to a fairly wide range of non-SSC conditions). Therefore any predictive function of SSC enhancement would be very limited in scope.

3.5 Suggestions for Future Research

The findings of this study offer interesting new directions for SSC research from both a muscle modelling perspective and for investigations of human performance factors. As mentioned in the previous section, current muscle models may be improved by investigating a wider range of SSC contractions. These investigations may reveal important relationships between the type of SSC movement (amplitude, velocity, coupling time...) and the magnitude of the various forms of SSC enhancement (neural potentiation, elastic recovery, exploitation of CC mechanics). These relationships may then be incorporated into existing muscle models to improve their predictive ability and to widen their scope of application. Ultimately, reliable models of muscle function will permit precise and comprehensive investigations of human movement phenomena to be performed through the use of computer simulations. In their developmental stages, these models offer a useful means of examining physiological phenomena

which can not be directly measured or which can not be adequately isolated experimentally.

From a human performance perspective, the ability to distinguish between the influences of different SSC phenomena could have a significant impact on movement techniques and on training methods. For example, it has been reported that the compliance of elastic structures in pig muscles is function dependent (Shadwick, 1990). That is, tendons of muscles which commmonly undergo SSCs were found to be stiffer, less extensible and acted as better energy storing structures than tendons of less heavily loaded muscles. Muscle models could allow indirect estimates of these types of phenomena in intact human systems. Because so many sporting skills involve SSCs, the impact of such investigations could prove very beneficial in assessing the effectiveness of specific training regimens.

3.5 Summary and Conclusions

The impact of the stretch-shortening cycle on human movement is well recognized, and series elastic recovery has been identified as an important contributor to its effects. The influence of series elastic recovery has nonetheless been difficult to assess in voluntary human movements because of the interacting influences of other neural and mechanical phenomena associated with SSCs. The modelling methods used in this study were able to account for the influences of these other SSC phenomena and thereby isolate the effects of series

elastic recovery. The results indicated that the bulk of the performance enhancement observed in the SSC contractions could be attributed to work performed by stored elastic energy. These findings provide added clarity to studies which have previously advocated the significance of elastic recovery in voluntary human movements. Nevertheless, it should not be concluded that elastic energy recovery is the sole or primary source of SSC enhancement. The relative contributions of the various neural and mechanical factors associated with SSCs are likely to depend largely on the characteristics of the task being performed. One very important finding that can be drawn from this study is that Hill-based muscle models provide a useful tool for assessing the influences of physiological phenomena on human movement performance. Particularly the influences of phenomena which can neither be directly measured nor experimentally controlled.

REFERENCES

Alexander, R. McN., & Bennet-Clark, H. C. (1977). Storage of elastic strain energy in muscle and other tissues. _Nature_, _265_, 114-117.

Amis, A. A., Dowson, D., & Wright, V. (1979). Muscle strengths and musculo-skeletal geometry of the upper limb. _Engineering in Medicine_, _8_, 41-48.

Asmussen, E., & Bonde-Petersen, F. (1974). Apparent efficiency and storage of elastic energy in human muscles during exercise. _Acta Physiologica Scandinavica_, _92_, 537-545.

Aura, O., & Komi, P. V. (1987). Coupling time in stretch-shortening cycle: Influence on mechanical efficiency and elastic characteristics of leg extensor muscles. In: B. Jonsson (Ed.), _Biomechanics X-A_ (pp. 507-511). Champaign, IL: Human Kinetics.

Bahler, A. S. (1967). Series elastic component of mammalian skeletal muscle. _American Journal of Physiology_, 213, 1560-1564.

Basmajian, J. V., & DeLuca, C. J. (1985). _Muscles Alive: Their Functions Revealed by Electromyography._ (5th ed.). Baltimore, MD: Williams & Wilkens.

Bigland-Ritchie, B. (1981). EMG/force relations and fatigue of human voluntary contractions. _Exercise and Sport Sciences Reviews_, _9_, 75-117.

Bobbert, M. F., & Van Ingen Schenau, G. J., (1988). Coordination in vertical jumping. _Journal of Biomechanics_, _21_, 249-262.

Bober, T., Jaskolski, E., & Nowacki, Z. (1980). Study on ecccentric-concentric contraction of the upper body extremity muscles. _Journal of Biomechanics_, _13_, 135-138.

Bosco, C., & Komi, P. V. (1979). Potentiation of the mechanical behaviour of muscle through pre-stretching. _Acta Physiologica Scandinavica_, _106_, 467-472.

Bosco, C., Viitasalo, J. T., & Komi, P. V. (1982). Combined effect of elastic energy and myoelectric potentiation during stretch-shortening cycle exercises. Acta Physiologica Scandinavica, 14, 559-565.

Bouisset, S., Lestienne, F., & Maton, B. (1977). The stability of synergy in agonists during the execution of a simple voluntary movement. Electroencephalography and Clinical Neurophysiology, 42, 543-551.

Caldwell, G. E., & Chapman, A. E. (1989). Applied muscle modelling: Implementation of muscle specific models. Computers in Biology and Medicine, 19(6), 417-434.

Cavagna, G. A. (1977). Storage and utilization of elastic energy in skeletal muscle. Exercise and Sport Science Reviews, 5, 89-127.

Cavagna, G. A., Dusman, B., & Margaria, R. (1968). Positive work done by previously stretched muscle. Journal of Applied Physiology, 24, 21-32.

Cavagna, G. A., & Kaneko, M. (1977). Mechanical work and efficiency in level walking and running. Journal of Physiology (London), 268, 467-481.

Cavagna, G. A., Saibene, F. P., & Margaria, R. (1964). Mechanical work in running. Journal of Applied Physiology, 19, 249-252.

Cavagna, G. A., Saibene, F. P., & Margaria, R. (1965). Effect of negative work on the amount of positive work performed by an isolated muscle. Journal of Applied Physiology, 20(1), 157-158.

Chapman, A. E., & Calvert, T. W. (1979). Estimation of active-state from E.M.G. recordings of human muscular contractions. Electromyography and Clinical Neurophysiology, 19, 199-222.

Chapman, A. E. (1985). The mechanical properties of human muscle. Exercise and Sport Science Reviews, 13, 443-501.

Chapman, A. E., & Sanderson, D. J. (1990). Muscular coordination in sporting skills. In: J.M. Winters and S.L-Y. Woo (Eds.), Multiple Muscle Systems: Biomechanics and Movement Organization (pp. 608-620) Springer-Verlag, U.S.A.

Close, R. I. (1972). Dynamic properties of mammalian skeletal muscles. <u>Physiological Reviews</u>, <u>52</u>, 129-197.

Dowling, J. J. (1987). <u>The Prediction of Force in Individual Muscles Crossing the Human Elbow Joint</u>. Ph.D. Dissertation, University of Waterloo, Waterloo, Ontario.

Dowling, J. J. (1992). The effect of muscle mechanics on human movement outcomes as revealed by computer simulation. <u>Human Movement Science</u>, <u>11</u>(3), 273-297.

Dul, J., Townsend, M. A., Shiavi, R., & Johnson, G. E. (1984). Muscular synergism - I: On criteria for load sharing between synergistic muscles. <u>Journal of Biomechanics</u>, <u>17</u>, 663-673.

Ettema, G. J. C. & Huijing, P. A. (1990). Architecture and elastic properties of the series elastic element of muscle tendon complex. In: J.M. Winters and S.L-Y. Woo (Eds.), <u>Multiple Muscle Systems: Biomechanics and Movement Organization</u> (pp. 57-68) Springer-Verlag, U.S.A.

Faulkner, J. A., Jones, D. A., Round, J. M., & Edwards, R. H. T. (1980). Dynamics of energetic processes in human muscle. In: P. Cerretelli and B.J. Whipp (Eds.), <u>Exercise Bioenergetics and Gas Exchange</u> (pp. 81-90) Biomedical Press, Elsevier/North-Holland.

Fenn, W. O. (1930). Frictional and kinetic factors in the work of sprint running. <u>American Journal of Physiology</u>, <u>92</u>, 582-611.

Frigo, C., & Pedotti, A. (1978). Determination of muscle length during locomotion. in: E. Asmussen and K. Jorgensen (eds.), <u>Biomechanics VI-A</u>, University Park Press, Baltimore: pp. 355-360.

Hatze, H. (1981). Estimation of myodynamic parameter values from observations on isometrically contracting muscle groups. <u>European Journal of Applied Physiology</u>, <u>46</u>, 325-338.

Hayes, K. C., & Hatze, H. (1976). Passive visco-elastic properties of the structures spanning the human elbow joint. <u>European Journal of Applied Physiology</u>, <u>37</u>, 265-274.

Henneman, E., Somjen, G., & Carpenter, D. O. (1965). Functional significance of cell size in spinal motoneurons. Journal of Neurophysiology, 28, 560-580.

Hill, A. V. (1950). The series elastic component of muscle. Proceedings of the Royal Society B (London), 137, 273-280.

Hill, A. V. (1970). First and Last Experiments in Muscle Mechanics, Cambridge University Press, Cambridge.

Hof, A. L., & Van de Berg, J. W. (1981a). EMG to force processing I: An electrical analogue of the Hill muscle model. Journal of Biomechanics, 14, 747-758.

Hof, A. L., & Van de Berg, J. W. (1981b). EMG to force processing IV: Eccentric-concentric contractions on a spring-flywheel set up. Journal of Biomechanics, 14, 787-792.

Hof, A. L., & Van de Berg, J. W. (1986). How much energy can be stored in human muscle elasticity. Human Movement Science, 5, 107-114.

Hof, A. L. (1990). Effects of muscle elasticity in walking and running. In: J.M. Winters and S.L-Y. Woo (Eds.), Multiple Muscle Systems: Biomechanics and Movement Organization (pp. 591-607) Springer-Verlag, U.S.A.

Ismail, H. M., & Ranatunga, K. W. (1978). Isometric tension development in a human skeletal muscle in relation to its working range of movement: The length-tension relationship of Biceps Brachii muscle. Experimental Neurology, 62, 595-604.

Komi, P. V. (1984). Physiological and biomechanical correlates of muscle function: Effects of muscle structure and stretch-shortening cycle on force and speed. Exercise and Sports Science Reviews, 12, 81-121.

Komi, P. V., & Bosco, C. (1978). Utilization of stored elastic energy in leg extensor muscle by men and women. Medicine and Science in Sports, 10, 261-265.

LeBozec C., Maton, B., & Cnockaert, J. C. (1980). The synergy of elbow extensor muscles during dynamic work in man, I: Elbow extension. European Journal of Applied Physiology, 44, 255-269.

Lloyd, B. B., & Zacks, R. M. (1972). The mechanical
     efficiency of treadmill running against a horizontal
     impeding force. Journal of Physiology (London), 223,
     355-373.

Marey, M., & Demeney, M. G. (1885). Locomotion humaine,
     mecaninisme du saut. Comptes Rendus de L'Academie des
     Sciences, 101, 489-494.

Milner-Brown, H. S., & Stein, R. B. (1975). The relation
     between the surface electromyogram and muscular force.
     Journal of Physiology (London), 246, 549-569.

Mungiole, M., & Winters, J. M. (1991). Factors affecting
     elastic energy recovery in stretch-shortening
     movements. Proceedings for the 15th Annual Meeting of
     the American Society of Biomechanics, 186-187.

Shadwick, R. E. (1990). Elastic energy storage in tendons:
     mechanical differences related to function and age.
     Journal of Applied Physiology. 68(3), 1033-1040.

Shorten, M. R. (1987). Muscle elasticity and human
     performance. Medicine and Sports Science, 25, 1-18.

Thomson, D. B., & Chapman, A. E. (1988). The mechanical
     response of active human muscle during and after
     stretch. European Journal of Applied Physiology, 57,
     691-697.

Thys, H., Cavagna, G. A., & Margaria, R. (1975). The role
     played by elasticity in an exercise involving movements
     of small amplitude. Pflugers Archives, 354, 281-286.

Thys, H., Farraggiana, T., & Margaria, R. (1972).
     Utilization of muscle elasticity in exercise. Journal
     of Applied Physiology, 32, 491-494.

Van Ingen Schenau, G. J. (1984). An alternative view of the
     concept of utilization of elastic energy in human
     movement. Human Movement Sciences, 3, 301-336.

Van Ingen Schenau, G. J. (1986). Elastic energy and muscle
     potentiation, a continuing discussion. Human Movement
     Sciences, 5, 115-121.

Wilson, G. J., Elliott, B. C., & Wood, G. A. (1991). The effect on performance of imposing a delay during a stretch-shorten cycle movement. Medicine and Science in Sports and Exercise, 23(3), 364-370.

Winter, D. A. (1979). Biomechanics of Human Movement. New York: Wiley.

Winters, J. M., & Stark, L. (1987). Muscle models: What is gained and what is lost by varying model complexity. Biological Cybernetics, 55, 403-420.

Winters, J. M. (1990). Hill-based muscle models: An engineering perspective. In: J.M. Winters and S.L-Y. Woo (Eds.), Multiple Muscle Systems: Biomechanics and Movement Organization (pp. 69-93) Springer-Verlag, U.S.A.

Zahalak, G. I. (1990). Modeling muscle mechanics and energetics. In: J.M. Winters and S.L-Y. Woo (Eds.), Multiple Muscle Systems: Biomechanics and Movement Organization (pp. 1-23) Springer-Verlag, U.S.A.

Appendix A

Moment Arm Equations

The following equations were adapted from Dowling
(1987) to describe the muscle moment arm lengths as
functions of joint angle. Moment arms (MA) were measured in
meters and joint angles (θ) in degrees.

$MA_{BRD}(\theta)$

$= 2.15E-02$ $\theta > 160$

$= 9.69E-02 - 4.77E-04\ \theta$ $49 < \theta < 160$

$= 7.61E-02 - 6.05E-05\ \theta$ $\theta < 49$

$MA_{BIC}(\theta)$

$= 2.00E-02$ $\theta > 146$

$= -9.99E-04 + 1.46E-03\ \theta - 1.242E-05\ \theta^2$
$+ 2.32E-08\ \theta^3$ $\theta < 146$

$MA_{TRI}(\theta)$

$= 5.77E-02 - 1.07E-03\ \theta + 3.43E-06\ \theta^2$ $\theta > 120$

$= 1.82E-03 - 3.84E-04\ \theta + 1.57E-06\ \theta^2$ $65 < \theta < 120$

$= -1.64E-02$ $\theta < 65$

$MA_{BRA}(\theta)$

$= 1.64E-02$ $\theta > 133$

$= 5.9E-03 + 8.2E-04\ \theta - 8.09E-06\ \theta^2$
$+ 1.9E-08\ \theta^3$ $\theta < 133$
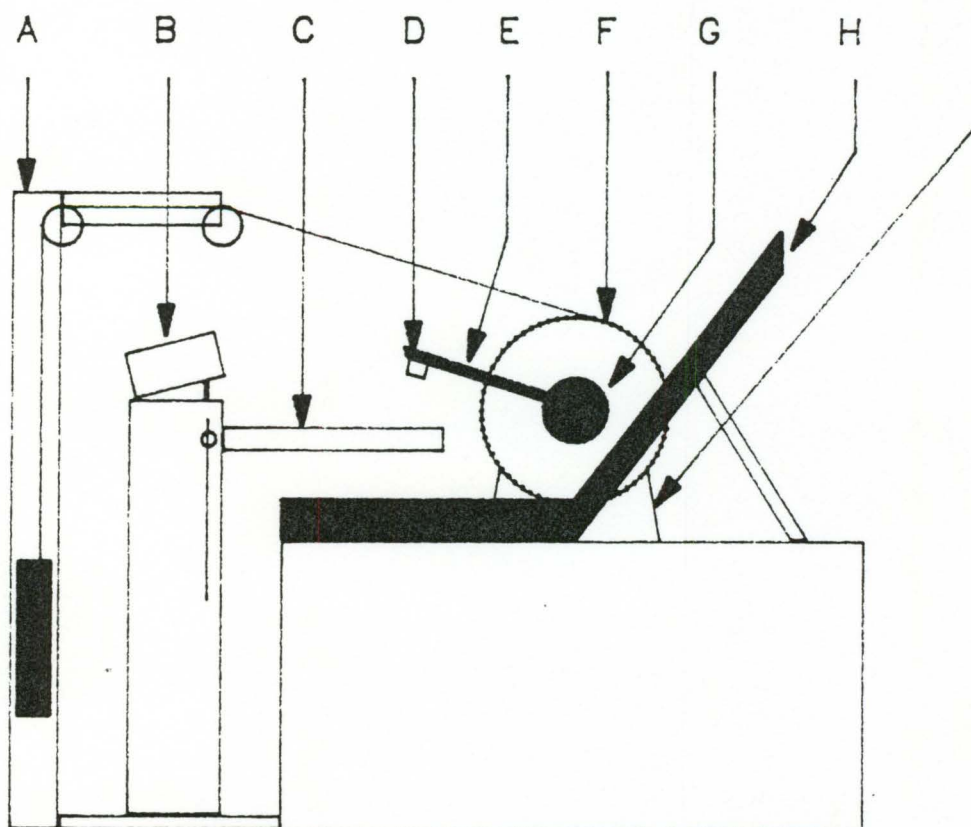
Whole Muscle Length Equations

The following equations were adapted from Dowling (1987) to describe whole muscle lengths as functions of joint angle. Muscle lengths (L) were measured in meters and joint angles (θ) in radians.

$$
\begin{aligned}
L_{BRD}(\theta) &= .273 + 2.15\text{E-}02\ \theta & \theta &> 2.80 \\
&= .1685 + 9.69\text{E-}02\ \theta - 1.367\text{E-}02\ \theta^2 & .86 < \theta &< 2.80 \\
&= .1776 + 7.61\text{E-}02\ \theta - 1.733\text{E-}02\ \theta^2 & \theta &< .86
\end{aligned}
$$

$$
\begin{aligned}
L_{BIC}(\theta) &= .331 + 2.00\text{E-}02\ \theta & \theta &> 2.55 \\
&= .292 - 9.91\text{E-}04\ \theta + 4.18\text{E-}02\ \theta^2 \\
&\quad - 1.359\text{E-}02\ \theta^3 + 1.091\text{E-}03\ \theta^4 & \theta &< 2.55
\end{aligned}
$$

$$
\begin{aligned}
L_{TRI}(\theta) &= .1574 + 5.77\text{E-}02 - 3.065\text{E-}02\ \theta^2 \\
&\quad + 3.75\text{E-}03\ \theta^3 & \theta &> 2.09 \\
&= .205 + 1.199\text{E-}03\ \theta - 1.046\text{E-}02\ \theta^2 \\
&\quad + 1.622\text{E-}03\ \theta^3 & 1.13 < \theta &< 2.09 \\
&= .214 - 1.648\text{E-}02\ \theta & \theta &< 1.13
\end{aligned}
$$

$$
\begin{aligned}
L_{BRA}(\theta) &= 9.41\text{E-}02 + 1.64\text{E-}02\ \theta & \theta &> 2.32 \\
&= 7.66\text{E-}02 + 5.9\text{E-}03\ \theta + 2.35\text{E-}02\ \theta^2 \\
&\quad - 8.85\text{E-}03\ \theta^3 + 8.93\text{E-}04\ \theta^4 & \theta &< 2.32
\end{aligned}
$$

Appendix B

Illustration of Apparatus

The following is a side view illustration of the apparutus used in the study. The subject, ELGON, EMG recording equipment, wires, amplifiers and A/D acquisition unit are not included for the sake of clarity.

A - weight & pulley system providing isotonic resistance.
B - oscilloscope
C - adjustable arm support
D - load cell
E - cybex arm assembly
F - chain wheel
G - torque transducer
H - Cybex chair
I - Cybex II Isokinetic Dynamometer